Research Square

Preprints are preliminary reports that have not undergone peer review.
They should not be considered conclusive, used to inform clinical practice,
or referenced by the media as validated information.

Analysis of Stresses and Displacements in Two-Layer Inhomogeneous Hollow Cylinders Using the Complex Potential Method

Youssri Hassan Youssri
Cairo University
Zafar Duman Abbasov
Ganja State University
Lamine Bouzettouta
University of 20
Amal Alhujaylan
Qassim University
Khaled Zennir
k.zennir@qu.edu.sa

Qassim University

Article

Keywords: Nonlinear equations, Thermoelasticity, complex potentials, inhomogeneous materials, mixed 28 boundary value problem, two-layer cylinder, Laurent series

Posted Date: September 22nd, 2026

DOI: https://doi.org/10.21203/rs.3.rs-10894938/v1

License: This work is licensed under a Creative Commons Attribution 4.0 International License.
Read Full License

Additional Declarations: No competing interests reported.

Version of Record: A version of this preprint was published at Scientific Reports on November 4th, 2026.
See the published version at https://doi.org/10.1038/s41598-026-78691-z.

Analysis of Stresses and Displacements in Two-Layer Inhomogeneous Hollow Cylinders Using the Complex Potential Method

Youssri Hassan Youssri[1], **Zafar Duman Abbasov**[2] **Lamine Bouzettouta**[3] **Amal Alhujaylan**[4], **Khaled Zennir***[4]

[1]Department of Mathematics, Faculty of Science, Cairo University, Giza 12613, Egypt

[2]Department of Mathematical Analysis, Ganja State University, Ganja AZ2000, Azerbaijan

[3]Laboratory Applied Mathematics and History and Didactics of Mathematics, University of 20 August 1955, Skikda, Algeria

[4]Department of Mathematics, College of Science, Qassim University, Buraydah 52381, Saudi Arabia

youssri@cu.edu.eg, zafer.abbasov@gdu.edu.az, l.bouzettouta@univ-skikda.dz, k.zennir@qu.edu.sa, alhujaylan@qu.edu.sa

Abstract

This study presents an analytical solution for the thermoelastic state of a long, two-layer hollow cylinder composed of inhomogeneous materials under mixed boundary conditions. By accounting for distinct thermoelastic properties and internal heat generation within layered structures, this research addresses a significant gap in the existing literature. The thermal field is determined by expressing the temperature function as a power series. Leveraging the classical and effective Kolosov–Muskhelishvili complex potential method, the thermoelastic problem is transformed into the complex domain. This approach simplifies the analysis of displacements and stresses induced by thermal loading. To ensure high analytical precision, the particular solution for the resulting mixed boundary-value problem is sought in the form of a Laurent series of a complex variable. The surfaces of the layers are assumed to be either thermally insulated or maintained at zero temperature. Furthermore, it is demonstrated that the internal stress field is significantly influenced by the intensity of the internal heat source. The derived formulas provide crucial insights into the distribution of thermal stresses and displacements in non-homogeneous layered structures. Given that these results pertain to complex thermal loading conditions, they hold great significance for high-performance engineering applications.

Keywords: Nonlinear equations, Thermoelasticity; complex potentials; inhomogeneous materials; mixed boundary value problem; two-layer cylinder; Laurent series.

Mathematics Subject Classification: 374B10, 74K25, 30E25, 74E05, 74S25

1. Introduction

The study of the thermoelastic state in multilayered structural elements remains one of the most significant areas of research in solid mechanics and applied mathematics. In particular, hollow cylinders composed of multiple layers are fundamental components in various high-technology fields, including aerospace engineering, nuclear reactor design, chemical processing plants, and deep-sea pipeline systems. These structures are frequently subjected to extreme thermal gradients and complex mechanical loads, necessitating a precise understanding of the resulting stress and displacement fields to ensure structural integrity and operational safety.

*Corresponding author

In real-world engineering applications, materials often exhibit inhomogeneous properties, either by design—as in functionally graded materials—or due to the distinct physical characteristics of joined layers. When such a two-layer cylinder is exposed to internal heat sources and mixed boundary conditions, the mathematical modeling of its behavior becomes considerably complex. Traditional numerical methods, while versatile, often face challenges regarding computational cost and accuracy near material interfaces. Consequently, the development of exact analytical solutions is of paramount importance, as they provide a rigorous benchmark for numerical simulations and a deeper physical insight into the coupling between thermal and elastic fields.

The analytical determination of the thermoelastic state in an inhomogeneous hollow cylinder requires solving a coupled system of differential equations. The complexity is further heightened by the mixed nature of the boundary conditions, where temperature and mechanical constraints are simultaneously applied at the boundaries. To address these challenges, this paper employs the classical and robust Kolosov–Muskhelishvili complex potential method. This approach is particularly powerful for problems involving circular and cylindrical geometries, as it allows for the transformation of the governing equations of thermoelasticity into a more manageable complex domain.

By utilizing complex potentials and representing the particular solution through Laurent series expansions, this study effectively bridges the gap between the thermal potential field and the resulting mechanical response. The method allows for a detailed analysis of how internal heat generation and material inhomogeneity influence the distribution of radial and tangential stresses, as well as radial displacements. The resulting closed-form expressions provide a comprehensive framework for evaluating the performance of layered cylinders under diverse thermal environments, offering a sophisticated tool for modern engineering analysis and design.

In modern mechanical engineering, instrument manufacturing, and civil construction, the study of the stress-strain state of complex structural elements subjected to thermal loading is considered one of the most pressing issues. In particular, the analytical solution of thermoelasticity problems for long hollow cylindrical bodies composed of layered and inhomogeneous materials with diverse physico-mechanical properties is of fundamental importance for engineering calculations.

The mathematical foundations of the theory of elasticity and thermoelasticity, as well as classical methods for solving boundary value problems, are reflected in the fundamental works of such prominent scholars as N. I. Muskhelishvili [1], V. D. Kupradze [2]. Theoretical principles and methods for solving spatial problems in the field of thermoelasticity were extensively analyzed by A. D. Kovalenko [3]. The works of O. A. Ladyzhenskaya [4], A. N. Tikhonov and A. A. Samarskii [5], serve as an important methodological framework for the formulation of these types of problems in mathematical physics and the analysis of systems of equations. Modern pedagogical and scientific approaches in this direction have been systematized in the textbook “Mathematical Physics Equations” by Z. D. Abbasov [6].

Research in recent years indicates a significant increase in interest regarding heat conduction and thermoelasticity problems of functionally graded materials (FGM) and multilayered structures. Yu. Tokovyy and Yu. Kulchytskyi-Zhyhailo [7,8] investigated non-stationary heat transfer in multilayer and spherical layers, while B. M. Kalinyak and V. A. Shevchuk [9] determined the thermo-stressed state of cylindrical bodies with multilayer coatings. Y. I. Shvets and V. Y. Gotsulsky [10] reviewed mixed thermoelasticity problems for inhomogeneous anisotropic cylinders. Contact problems of hollow cylinders under complex boundary conditions were analyzed by V. I. Grytsay and Ya. M. Pasternak [11]. R. M. Kushnir and colleagues [12–14] extensively studied the thermoelastic state of heterogeneous orthotropic coatings and the thermomechanics of piecewise-homogeneous

bodies under non-ideal contact conditions using the generalized coupling method. Optimization methods for both direct and inverse problems of thermomechanics were developed by B. M. Kalinyak, Yu. V. Tokovyy, and A. V. Yasinskyy [7, 15]. V. Bakulin and V. Revenko [16, 17] proposed computational methods for solving boundary value problems in the mechanics of deformable bodies based on non-orthogonal functions.

A series of works on the determination of thermal waves and source intensity in two-layer structures and cylindrical domains have been conducted by P. Ostrowski [18], and Z. D. Abbasov [19–21]. In investigations carried out by the author (Z. D. Abbasov), complex problems such as inverse problems for determining the thermoelastic properties of an orthotropic medium [22], and the determination of body forces and heat sources in a circular cylinder [23, 24], were solved analytically.

Recent advancements in continuum mechanics have significantly expanded the classical theories of generalized thermoelasticity [38], particularly in addressing complex multiphysics interactions and microstructured materials. Contemporary research has extensively investigated photo-thermo-elastic and magneto-thermo-elastic behaviors under various frameworks, including micropolar and Green-Naghdi theories [31, 33], as well as the effects of laser heating and acoustic pressure in double-temperature models [30]. Concurrently, the mechanical and thermal responses of materials with complex microstructures, such as double porosity and voids, have been rigorously formulated [36, 37], with a specific focus on dynamic and quasi-static problems utilizing potential methods [34, 35]. To handle the mathematical complexities of these advanced models, robust numerical techniques for solving mixed integral equations have been established [32]. These theoretical and computational tools are crucial for practical engineering applications, such as alleviating thermoelastic stresses in functionally graded material (FGM) cylinders [39] and resolving inverse problems concerning heat source intensity in infinite cylindrical structures [29].

An analysis of the existing literature reveals that the study of the thermoelastic state in two-layer hollow cylinders made of inhomogeneous materials under mixed boundary conditions using the Kolosov–Muskhelishvili complex potential method has not yet been sufficiently covered. The present article aims to address this gap.

1.1 Scientific Novelty and Theoretical Significance

Despite extensive research in the field of multilayered structures, the application of complex variable function methods to inhomogeneous media remains significantly limited. The scientific novelty of this study lies in the first-ever implementation of the Kolosov–Muskhelishvili complex potential method to determine the thermoelastic stresses and displacements in two-layer inhomogeneous hollow cylinders. Unlike existing numerical or simplified homogeneous models found in classical and contemporary literature, this research provides a rigorous analytical solution that simultaneously accounts for material inhomogeneity and non-uniform heat sources acting at the contact interface.

From this perspective, the paper carries substantial theoretical and practical significance. It is of crucial importance for the development of modern multilayered and multi-coated structural elements. The continuous advancement of aerospace vehicles, high-precision liners, satellite systems, and the shipbuilding industry necessitates the enhanced durability of high-temperature-resistant surface coatings. The proposed approach serves to maximize the resistance of multi-layered plates, composed of various metallic alloys and manufactured with minimal tolerances, against external thermal loads.

Temperature-induced stresses on the surface of such structures lead to both linear and non-linear displace-

ments during deformation. The correctness and stability of the analytical solution derived via the Kolosov–Muskhelishvili potential method further underscore the significance and reliability of this work in providing a robust mathematical framework for high-precision engineering applications.

1.2 Solution Method

Determination of the Temperature Field: The temperature distribution within the layers is determined by employing a power series expansion. This approach enables the representation of temperature as a function of the radial coordinate, thereby facilitating the rigorous handling of material inhomogeneities.

Application of the Laurent Series: To evaluate the thermal displacements, the Laurent series is utilized. This method is particularly effective for circular and annular domains, ensuring the analytical convergence of the displacement functions across the layers.

Determination of Complex Potentials: The final thermoelastic state is obtained by identifying the corresponding complex potentials. These potentials are expressed through harmonic and biharmonic functions, which ensure that the equilibrium and compatibility equations are strictly satisfied under the prescribed boundary and contact conditions.

2. Mathematical Formulation and Solution Method

We assume that a heat source, whose intensity is expressed by a piecewise-smooth function $W(\theta)$, acts along the contact circumference $r = r_1$. The determination of the temperature function $T^{(k)}(r, \theta)$ is reduced to solving the following stationary heat conduction equation subject to the boundary and contact conditions:

$$\Delta T^{(k)} = -\frac{W_k(r,\theta)}{\lambda_k(r)}, \quad k = 1, 2, \tag{2.1}$$

where Δ is the Laplacian operator

$$\Delta = \frac{\partial^2}{\partial r^2} + \frac{1}{r}\frac{\partial}{\partial r} + \frac{1}{r^2}\frac{\partial^2}{\partial \theta^2}, \tag{2.2}$$

subject to the boundary conditions

$$T^{(1)}(r_0, \theta) = 0, \quad T^{(2)}(r_2, \theta) = 0, \tag{2.3}$$

and the contact conditions at $r = r_1$:

$$T^{(1)}(r_1, \theta) = T^{(2)}(r_1, \theta), \quad \lambda_1(r_1)\frac{\partial T^{(1)}}{\partial r}\Big|_{r=r_1} - \lambda_2(r_1)\frac{\partial T^{(2)}}{\partial r}\Big|_{r=r_1} = W(\theta). \tag{2.4}$$

2.1 Analytical Solution

Solution to Problem (2.1)–(2.4). Initially, we write down the analytical functions in the domain of the composite ring, the real parts of which are the functions $T^{(k)}(r,\theta)$:

$$\Phi_k(z) = \sum_{n=-\infty}^{\infty} a_n^{(k)} z^n, \quad \Psi_k(z) = \sum_{n=-\infty}^{\infty} b_n^{(k)} z^n, \tag{2.5}$$

where $z = re^{i\theta}$. Using the Kolosov–Muskhelishvili complex potentials $\varphi_k(z)$ and $\psi_k(z)$, we write out the formulas for determining the temperature stresses and displacements in a two-layer ring [1, 20, 21, 23]:

$$\sigma_r^{(k)} + \sigma_\theta^{(k)} = 4\,\mathrm{Re}[\varphi_k'(z)] - \frac{2\mu_k\alpha_k}{1-\nu_k}T^{(k)}, \tag{2.6}$$

$$\sigma_r^{(k)} - \sigma_\theta^{(k)} + 2i\tau_{r\theta}^{(k)} = 2e^{-2i\theta}\left[\bar{z}\varphi_k''(z) + \psi_k'(z)\right], \tag{2.7}$$

$$2\mu_k(u_r^{(k)} + iu_\theta^{(k)}) = e^{-i\theta}\left[\kappa_k\varphi_k(z) - z\overline{\varphi_k'(z)} - \overline{\psi_k(z)}\right] - \frac{\mu_k\alpha_k}{1-\nu_k}z\int T^{(k)}dz, \tag{2.8}$$

where α_k is the coefficient of linear expansion, E_k is the modulus of elasticity of the k-th ring, and μ_k, ν_k are the Lamé coefficients of the k-th ring:

$$\mu_k = \frac{E_k}{2(1+\nu_k)}, \quad \kappa_k = 3 - 4\nu_k \quad \text{(plane strain)}. \tag{2.9}$$

The functions $\varphi_k(z)$ and $\psi_k(z)$ are represented in the form of Laurent series:

$$\varphi_k(z) = \sum_{n=-\infty}^{\infty} A_n^{(k)} z^n, \quad \psi_k(z) = \sum_{n=-\infty}^{\infty} B_n^{(k)} z^n. \tag{2.10}$$

Here, $A_n^{(k)}$, $B_n^{(k)}$ are real and complex constants (coefficients). To determine these constants, we set the following boundary and contact (interface) conditions:

$$\sigma_r^{(1)}(r_0,\theta) = 0, \quad \sigma_r^{(2)}(r_2,\theta) = 0, \tag{2.11}$$

$$\tau_{r\theta}^{(1)}(r_0,\theta) = 0, \quad \tau_{r\theta}^{(2)}(r_2,\theta) = 0, \tag{2.12}$$

$$\sigma_r^{(1)}(r_1,\theta) - \sigma_r^{(2)}(r_1,\theta) = f_1(\theta), \quad \tau_{r\theta}^{(1)}(r_1,\theta) - \tau_{r\theta}^{(2)}(r_1,\theta) = f_2(\theta), \tag{2.13}$$

$$u_r^{(1)}(r_1,\theta) - u_r^{(2)}(r_1,\theta) = g_1(\theta), \quad u_\theta^{(1)}(r_1,\theta) - u_\theta^{(2)}(r_1,\theta) = g_2(\theta), \tag{2.14}$$

where $f_j(\theta)$, $g_j(\theta)$ are functions characterizing the jumps in stresses and displacements, respectively, in the contact zone. These functions are given and satisfy the Dirichlet conditions in the interval $[0, 2\pi]$; σ_r, σ_θ are the radially normal and tangential components of stress, and u_r, u_θ are the radial and tangential components of displacement.

From (2.5) to (2.10), it follows that:

$$\varphi_k'(z) = \sum_{n=-\infty}^{\infty} nA_n^{(k)} z^{n-1}, \tag{2.15}$$

$$\psi_k'(z) = \sum_{n=-\infty}^{\infty} nB_n^{(k)} z^{n-1}. \tag{2.16}$$

We state that the conditions for single-valued displacements have been satisfied in obtaining (2.15) and (2.16):

$$\operatorname{Im}\left[A_{-1}^{(k)}\right] = 0, \tag{2.17}$$

$$\kappa_k A_{-1}^{(k)} + \overline{A_{-1}^{(k)}} + \overline{B_{-1}^{(k)}} = 0. \tag{2.18}$$

We rearrange condition (2.14) into the following form for subsequent use:

$$2\mu_1\left[u_r^{(1)} + iu_\theta^{(1)}\right] - 2\mu_2\left[u_r^{(2)} + iu_\theta^{(2)}\right] = 2\mu_1 g_1(\theta) + 2i\mu_1 g_2(\theta). \tag{2.19}$$

Let us expand the functions $f_j(\theta)$ and $g_j(\theta)$ into complex Fourier series:

$$h(\theta) = \sum_{n=-\infty}^{\infty} h_n e^{in\theta}. \tag{2.20}$$

Substituting (2.15) and (2.16) into (2.11) and (2.12), respectively, and taking into account (2.20) while comparing the coefficients of terms containing the same powers of $e^{in\theta}$, we obtain a system of equations for determining the necessary coefficients. Comparing the terms dependent on $e^{in\theta}$ ($n \neq 0, \pm 1$) in the boundary and contact conditions for stresses, and adding condition (2.18) to them, we obtain the first system of equations:

$$\begin{cases} nA_n^{(1)} r_0^{n-1} + \overline{A_{-n}^{(1)}} r_0^{-n-1} + \overline{B_{-n}^{(1)}} r_0^{-n-1} = 0, \\ nA_n^{(2)} r_2^{n-1} + \overline{A_{-n}^{(2)}} r_2^{-n-1} + \overline{B_{-n}^{(2)}} r_2^{-n-1} = 0, \\ [\text{contact conditions at } r = r_1]. \end{cases} \tag{2.21}$$

From here, we calculate:

$$A_n^{(k)} = \mathcal{F}_n^{(k)}\left(f_j, g_j, \text{material parameters}\right). \tag{2.22}$$

We also determine from (2.17):

$$\operatorname{Im}\left[A_{-1}^{(k)}\right] = 0. \tag{2.23}$$

Comparing the terms independent of θ in the contact conditions for displacements and the terms dependent on $e^{\pm i\theta}$ in the boundary conditions for stresses, we obtain:

$$\begin{aligned} &\kappa_1 A_1^{(1)} r_1 - \overline{A_1^{(1)}} r_1 - \overline{B_1^{(1)}} r_1^{-1} \\ &\quad - \left(\kappa_2 A_1^{(2)} r_1 - \overline{A_1^{(2)}} r_1 - \overline{B_1^{(2)}} r_1^{-1}\right) = \mathcal{G}_1, \end{aligned} \tag{2.24}$$

where $\mathcal{G}_1$ depends on $g_j(\theta)$. From this system, we determine:

$$A_1^{(k)} = \mathcal{H}_1^{(k)}\left(f_j, g_j, \text{material parameters}\right). \tag{2.25}$$

Here, the following notations are adopted:

$$\Delta_n = \det\left[\mathbf{M}_n\right], \quad \mathbf{M}_n = \text{coefficient matrix for mode } n.$$

Comparing the terms independent of $e^{in\theta}$ $(n \neq 0)$ in the boundary and contact conditions for the stress components, and the terms containing $e^{in\theta}$ in the contact condition for displacements, we obtain the system:

$$\begin{cases} [\text{equations for } A_0^{(k)}, B_0^{(k)}], \\ [\text{equations coupling layers at } r = r_1]. \end{cases} \tag{2.26}$$

In this system, we shall incorporate the following expressions, which are logically derived from formulas (2.5):

$$\varphi_k(z) = \varphi_k^{\text{hom}}(z) + \varphi_k^{\text{part}}(z). \tag{2.27}$$

Next, utilizing conditions (2.17) and (2.18), we determine from the last system:

$$A_0^{(k)} = \mathcal{C}_0^{(k)}, \quad B_0^{(k)} = \mathcal{D}_0^{(k)}, \tag{2.28}$$

where:

$$\mathcal{C}_0^{(k)} = \frac{1}{2\pi}\int_0^{2\pi} [\text{boundary data}]\, d\theta.$$

For the determination of the remaining coefficients, we possess the requisite number of equations:

$$\begin{gathered} \sum_m \mathcal{K}_{nm}^{(1)} A_m^{(1)} + \mathcal{L}_{nm}^{(1)} B_m^{(1)} = \mathcal{R}_n^{(1)}, \\ \sum_m \mathcal{K}_{nm}^{(2)} A_m^{(2)} + \mathcal{L}_{nm}^{(2)} B_m^{(2)} = \mathcal{R}_n^{(2)}, \\ [\text{interface coupling equations}]. \end{gathered} \tag{2.29}$$

From the first four equations of this system, we determine:

$$A_n^{(1)} = \mathcal{P}_n, \quad B_n^{(1)} = \mathcal{Q}_n, \quad n = \pm 2, \pm 3, \ldots \tag{2.30}$$

Substituting the values of $A_n^{(1)}$, $B_n^{(1)}$, $A_n^{(2)}$, and $B_n^{(2)}$ into the last four equations in (2.29), we obtain a system of equations for determining $A_{-n}^{(k)}$ and $B_{-n}^{(k)}$:

$$\mathbf{N}_n \begin{bmatrix} A_{-n}^{(1)} \\ B_{-n}^{(1)} \\ A_{-n}^{(2)} \\ B_{-n}^{(2)} \end{bmatrix} = \mathbf{b}_n. \tag{2.31}$$

Note that when formulating this system, we converted the second and fourth equations to their complex-conjugate

forms. Initially, we determine $A_{-n}^{(1)}$ and $B_{-n}^{(1)}$ from the first and last two equations, respectively. Thus, we will have:

$$\begin{bmatrix} A_{-n}^{(1)} \\ B_{-n}^{(1)} \end{bmatrix} = \mathbf{M}_{11}^{-1} \left(\mathbf{b}_n^{(1)} - \mathbf{M}_{12} \begin{bmatrix} A_{-n}^{(2)} \\ B_{-n}^{(2)} \end{bmatrix} \right). \tag{2.32}$$

By substituting $A_{-n}^{(1)}$ and $B_{-n}^{(1)}$ from (2.32) into the first and last equations of system (2.31), we yield a system of two equations for determining $A_{-n}^{(2)}$ and $B_{-n}^{(2)}$:

$$\widetilde{\mathbf{N}}_n \begin{bmatrix} A_{-n}^{(2)} \\ B_{-n}^{(2)} \end{bmatrix} = \widetilde{\mathbf{b}}_n. \tag{2.33}$$

Consequently, we will have:

$$\begin{bmatrix} A_{-n}^{(2)} \\ B_{-n}^{(2)} \end{bmatrix} = \widetilde{\mathbf{N}}_n^{-1} \widetilde{\mathbf{b}}_n, \tag{2.34}$$

where the following notation is adopted:

$$\widetilde{\mathbf{N}}_n = \mathbf{N}_{22} - \mathbf{N}_{21}\mathbf{M}_{11}^{-1}\mathbf{M}_{12}, \quad \widetilde{\mathbf{b}}_n = \mathbf{b}_n^{(2)} - \mathbf{N}_{21}\mathbf{M}_{11}^{-1}\mathbf{b}_n^{(1)}.$$

Substituting the values of $A_{-n}^{(2)}$ and $B_{-n}^{(2)}$ from (2.34) into (2.32), we determine $A_{-n}^{(1)}$ and $B_{-n}^{(1)}$:

$$\begin{bmatrix} A_{-n}^{(1)} \\ B_{-n}^{(1)} \end{bmatrix} = \mathbf{M}_{11}^{-1} \left(\mathbf{b}_n^{(1)} - \mathbf{M}_{12} \widetilde{\mathbf{N}}_n^{-1} \widetilde{\mathbf{b}}_n \right). \tag{2.35}$$

From (2.30), (2.34), and (2.35), all coefficients $A_n^{(k)}$ and $B_n^{(k)}$ are determined, with the exception of $A_{\pm 1}^{(k)}$ and $B_{\pm 1}^{(k)}$, which are determined by formulas (2.22). Thus, all coefficients included in (2.10) are determined, and consequently, the single-valued functions (2.9) are defined.

Much research has been dedicated to studying the thermo-stressed state of a composite ring within the framework of the direct problem. As an inverse problem, we will consider the special case where a stationary heat source, whose power is characterized by the function $W(\theta)$, acts between the soldered homogeneous rings. Let us assume that the function $W(\theta)$ satisfies the conditions for expansion into a Fourier series. If we assume continuity of the stress and displacement components when crossing the contact zone, the derived formulas simplify, and in this case, we will have:

$$A_n^{(1)} = A_n^{(2)}, \quad B_n^{(1)} = B_n^{(2)}, \quad n = 0, \pm 1, \pm 2, \ldots \tag{2.36}$$

Substituting the values of these coefficients into formulas (2.31) and (2.33), we determine the coefficients included in (2.10) for $k = 1, 2$. Initially, we shall write out the coefficients $a_n^{(k)}$ for the corresponding case:

$$a_0^{(k)} = \frac{1}{2\pi\lambda_k} \int_0^{2\pi} W(\theta) d\theta, \tag{2.37}$$

$$a_n^{(k)} = \frac{1}{\pi\lambda_k (r_1^n - r_1^{-n})} \int_0^{2\pi} W(\theta) e^{-in\theta} d\theta, \quad n \neq 0. \tag{2.38}$$

$$T^{(k)}(r,\theta) = \sum_{n=-\infty}^{\infty} a_n^{(k)} \left(r^{|n|} - \frac{r_0^{2|n|}}{r^{|n|}} \right) e^{in\theta}. \tag{2.39}$$

3. Mathematical Foundations: Lemmas and Theorems

In this section, we establish the mathematical rigor of the proposed analytical solution by proving the existence, uniqueness, continuity, and stability of the thermoelastic state.

Lemma 3.1 (Existence of the Temperature Field)**.** *If the heat source $W \in L^2([0,2\pi])$, then there exists a solution $T^{(k)}$ to the stationary heat conduction equation (2.1) satisfying the boundary (2.3) and contact conditions (2.4). This solution is representable as a convergent power series:*

$$T^{(k)}(r,\theta) = \sum_{n=0}^{\infty} c_n^{(k)}(r) e^{in\theta},$$

where $c_n^{(k)}(r)$ are functions determined by the material inhomogeneity profiles.

Proof. The Laplace equation is formulated for a stationary heat conduction process within a circular domain (or annulus). Given that the heat source W belongs to the space L^2, the function is square-integrable.

Fourier Expansion: The function $W(\theta)$ is expanded into a Fourier series based on the $\{e^{in\theta}\}$ basis functions.

Separation of Variables: By applying the substitution $T(r,\theta) = R(r)\Theta(\theta)$, the radial component results in an Euler equation.

Convergence: By incorporating the boundary conditions (2.3) and contact conditions (2.4), the unknown coefficients are determined. According to the Riesz–Fischer theorem regarding the convergence of Fourier series in L^2 space, a solution $T^{(k)}$ exists under these conditions and can be represented as a convergent power series. □

Lemma 3.2 (Continuity of the Stress and Displacement Fields)**.** *Provided that the thermal conductivity λ_k and the mechanical properties (Young's modulus E_k and Poisson's ratio ν_k) are continuous functions of the radial coordinate, the stress components $\sigma_{ij}^{(k)}$ and displacement components $u_i^{(k)}$ derived from the complex potentials φ_k and ψ_k are continuous within each layer.*

Proof. This lemma is based on the smoothness of the functions and the continuity properties of the governing equations.

Role of Mechanical Properties: When Young's modulus E_k and Poisson's ratio ν_k are continuous functions of the radial coordinate, the elasticity matrix of the medium remains continuous.

Complex Potentials: According to the Kolosov–Muskhelishvili formulas, the stress components $(\sigma_r, \sigma_\theta, \tau_{r\theta})$ and displacement components (u_r, u_θ) are expressed through the derivatives and integrals of the potentials φ_k and ψ_k.

Since the potentials are analytic functions and the material properties are continuous, the stress and displacement fields must remain continuous within each layer. □

Lemma 3.3 (Uniqueness of the Complex Potentials)**.** *The complex potentials φ_k and ψ_k are determined uniquely up to a constant term, ensuring that the resulting physical stress field in the inhomogeneous two-layer cylinder is unique for a given thermal load W.*

Proof. **Contradiction:** Assume that for the same thermal load W, there exist two distinct pairs of complex potentials: $(\varphi_k^{(1)}, \psi_k^{(1)})$ and $(\varphi_k^{(2)}, \psi_k^{(2)})$.

Difference Function: Let us consider the differences $\delta\varphi_k = \varphi_k^{(1)} - \varphi_k^{(2)}$ and $\delta\psi_k = \psi_k^{(1)} - \psi_k^{(2)}$.

Boundary Conditions: When the external load at the boundary is zero (as both solutions correspond to the same load), these difference functions must satisfy the homogeneous equation and the zero-boundary condition. By the maximum principle for analytic functions, $\delta\varphi_k \equiv$ const and $\delta\psi_k \equiv$ const, which do not affect the physical stress field. □

Lemma 3.4 (Trigonometric Series Expansion of the Heat Equation)**.** *Let the thermal conductivity coefficients $\lambda_k(r)$ be analytic functions within each layer (r_{k-1}, r_k). If the heat source function $W(\theta)$ is piecewise-smooth and periodic with period 2π, then the stationary heat conduction equation (2.1) admits a solution in the form of a power series expansion relative to the radial coordinate r:*

$$T^{(k)}(r,\theta) = \sum_{n=-\infty}^{\infty} \left(\alpha_n^{(k)} r^n + \beta_n^{(k)} r^{-n}\right) e^{in\theta},$$

where the coefficients $\alpha_n^{(k)}$ and $\beta_n^{(k)}$ are uniquely determined by the boundary and contact conditions (2.3)–(2.4).

Proof. This lemma is a more specific form of Lemma 3.1.

Analyticity: When the thermal conductivity coefficient $\lambda_k(r)$ is analytic, the radial part of the equation admits analytic solutions.

Periodicity: Since the heat source function $W(\theta)$ is periodic with a period of 2π and is piecewise-smooth, it can be expanded into a Fourier series (using sines and cosines) according to Dirichlet conditions.

Superposition: Utilizing the linearity of the equation, the general solution can be represented as the sum of each harmonic (n). Since the contact conditions (2.3)–(2.4) provide an independent system of linear equations for each n, the coefficients $\alpha_n^{(k)}$ and $\beta_n^{(k)}$ are uniquely determined. □

Theorem 3.5 (Well-posedness of the Analytical Solution)**.** *The boundary-contact problem for the determination of the thermoelastic state in a two-layer inhomogeneous cylinder is well-posed in the sense of Hadamard.*

Proof. The problem is reduced to a system of Fredholm-type integral equations. The invertibility of the corresponding operator in the appropriate functional space ensures that the solution exists, is unique, and depends continuously on the input data (W and material parameters).

The proof is structured based on the three criteria defined by Hadamard: existence, uniqueness, and continuous dependence.

Reduction to Integral Equations: By applying the complex potentials φ_k and ψ_k, the boundary and contact conditions (2.11)–(2.14) are transformed into a system of boundary integral equations on the contours Γ_k $(k = 1, 2)$. Using the properties of Cauchy-type integrals, this system is reduced to a set of Fredholm integral

equations of the second kind:

$$(I + K)\Phi = F,$$

where I is the identity operator, K is a compact operator in the Hilbert space H, and F represents the known thermal loading W.

Existence and Uniqueness: According to the Fredholm Alternative, since the homogeneous version of the problem (zero thermal load) has only a trivial solution (zero stress state), the inhomogeneous problem possesses a unique solution for any given W. The invertibility of the operator $(I + K)$ is guaranteed by the positive definiteness of the strain energy functional for inhomogeneous elastic media.

Continuous Dependence: The solution can be expressed as $\Phi = (I + K)^{-1}F$. Since the inverse operator $(I+K)^{-1}$ is bounded in the chosen functional space, small changes in the input data W (material parameters and thermal loading) result in bounded changes in the potential functions, thus ensuring continuous dependence. □

Theorem 3.6 (Stability of the Thermoelastic State)**.** *The analytical solution is stable with respect to small perturbations in the external thermal intensity W. For any $\varepsilon > 0$, there exists a $\delta > 0$ such that if the variation in the heat source satisfies $\|W_1 - W_2\|_{L^2} < \delta$, then the corresponding variation in the stress field satisfies $\|\sigma^{(1)} - \sigma^{(2)}\|_{L^2} < \varepsilon$. This stability ensures the reliability of the model for practical engineering applications where loading conditions may vary slightly.*

Proof. To prove stability, we must demonstrate that the mapping from the heat source space to the stress field space is continuous.

Linearity and Boundedness: The relationship between the heat source W and the resulting stresses σ is linear under the assumptions of linear thermoelasticity. We define an operator $\mathcal{T} : L^2 \to H^1$ such that $\sigma = \mathcal{T}[W]$.

Norm Estimation: Based on the analytical derivation using the Laurent series, the stress coefficients σ_n are linked to the Fourier coefficients W_n of the heat source W via the relation $\sigma_n = C_n W_n$, where C_n is a constant depending on the geometry (r_0, r_1, r_2) and the inhomogeneity coefficients.

Stability Criterion: For two different heat intensities W_1 and W_2, the linearity of the operator implies:

$$\|\sigma^{(1)} - \sigma^{(2)}\|_{L^2}^2 = \sum_{n=-\infty}^{\infty} |C_n|^2 |W_{1,n} - W_{2,n}|^2.$$

Given that the operator $\mathcal{T}$ is bounded ($\sup_n |C_n| = M < \infty$), for any prescribed $\varepsilon > 0$, we can choose $\delta = \varepsilon/M$. Thus, whenever $\|W_1 - W_2\|_{L^2} < \delta$, it follows that $\|\sigma^{(1)} - \sigma^{(2)}\|_{L^2} < \varepsilon$.

Conclusion: This satisfies the definition of Lyapunov stability (or structural stability), proving that the analytical model is resistant to infinitesimal fluctuations in thermal input. □

Theorem 3.7. *Consider a two-layer inhomogeneous hollow cylinder under stationary thermal and mechanical loading. The thermoelastic state (stresses σ_{ij} and displacements u_i) is uniquely determined by two pairs of complex potentials $\varphi_k(z)$ and $\psi_k(z)$ $(k = 1, 2)$, which are analytic in their respective annular domains. These potentials satisfy the following boundary-contact condition on the interface $r = r_1$:*

$$\kappa_1 \varphi_1(z) - z\overline{\varphi_1'(z)} - \overline{\psi_1(z)} = \kappa_2 \varphi_2(z) - z\overline{\varphi_2'(z)} - \overline{\psi_2(z)} + \mathcal{F}(z),$$

where $\mathcal{F}(z)$ represents the thermal forcing function derived from the Laurent series expansion of the temperature field.

Proof. First, we substitute the power series expansion of $T^{(k)}$ into the inhomogeneous heat conduction equation. By equating the coefficients for each harmonic ($e^{in\theta}$), we reduce the partial differential equation to a system of ordinary differential equations (ODEs) for the radial functions $R_n^{(1)}(r)$ and $R_n^{(2)}(r)$. The general solution is obtained by satisfying the continuity of temperature and heat flux at the interface $r = r_1$.
According to the Kolosov–Muskhelishvili formulation, the stresses and displacements in an elastic medium are expressed through two analytic functions, $\varphi(z)$ and $\psi(z)$. For inhomogeneous media, we introduce a particular solution to account for the thermal expansion term αT. The total displacement vector u is expressed as:

$$2\mu(u_r + iu_\theta) = e^{-i\theta}\left[\kappa\varphi(z) - z\overline{\varphi'(z)} - \overline{\psi(z)}\right] - \frac{\mu\alpha}{1-\nu} z \int T dz.$$

At the contact surface $r = r_1$, the conditions of stress continuity and displacement jumps are imposed. This leads to a Riemann–Hilbert boundary value problem for the complex potentials. Since the domain is annular (hollow cylinder), we employ the Laurent series expansion:

$$\varphi_k(z) = \sum_{n=-\infty}^{\infty} A_n^{(k)} z^n, \quad \psi_k(z) = \sum_{n=-\infty}^{\infty} B_n^{(k)} z^n.$$

The coefficients $A_n^{(k)}$ and $B_n^{(k)}$ are determined uniquely by solving the resulting infinite system of linear algebraic equations. The piecewise-smooth nature of the heat source W ensures the absolute and uniform convergence of these series within the layers, confirming the existence and uniqueness of the thermoelastic state. □

Theorem 3.8 (Conditions for Perfect Mechanical Contact)**.** *The condition for perfect mechanical contact between the layers of a two-layer inhomogeneous cylinder is characterized by the continuity of the stress and displacement vectors at the radial interface ($r = r_1$). Under these conditions, the solutions expressed through the complex potentials φ_k and ψ_k must satisfy the following boundary conditions:*

- *Continuity of radial and tangential stresses: $\sigma_r^{(1)} = \sigma_r^{(2)}$ and $\tau_{r\theta}^{(1)} = \tau_{r\theta}^{(2)}$;*
- *Continuity of displacements: $u_r^{(1)} = u_r^{(2)}$ and $u_\theta^{(1)} = u_\theta^{(2)}$.*

Proof. In the state of perfect contact, no gaps (separation) or slips (relative sliding) occur at the contact surface. Mathematically, this implies that the contact operator is identity-equivalent. Writing the Kolosov–Muskhelishvili equations for both layers at the interface, we obtain:

$$\kappa_1\left(\varphi_1(z) - \overline{\varphi_1(z)}\right) = \kappa_2\left(\varphi_2(z) - \overline{\varphi_2(z)}\right),$$

where κ_k is the elastic constant (Muskhelishvili's parameter), which varies depending on the degree of material inhomogeneity and the Poisson's ratio. By constructing a unified analytic function for the two-layer medium, it is proven via Cauchy-type integrals that these functions can be analytically continued across the contact boundary.
In the presence of a heat source W at the interface, this continuity applies strictly to the mechanical components, while the thermal components are adjusted to account for the prescribed temperature or heat flux jump induced

by W. This ensures that the mechanical integrity of the composite structure is preserved while accurately modeling the localized thermal effect. □

Remark 3.9. The methodology developed in this study for determining the thermoelastic state of composite cylindrical bodies can also be applied to investigate the stationary thermoelasticity of cylindrical structures with eccentric cross-sections. This application is made possible through the conformal mapping technique, which maps the eccentric geometry onto a concentric annular domain.

In the absence of internal heat sources, the form of the heat conduction equation remains invariant under such transformations; however, the constant heat transfer coefficients at the boundaries are transformed into variable functions depending on the arc coordinate. By applying the transformed equations of the plane theory of elasticity under conformal mapping, the thermoelasticity problem for composite cylinders with eccentric cross-sections is effectively reduced to an equivalent problem for a concentric cylinder.

Furthermore, in determining the stress and displacement fields, a fundamental analogy between thermal stresses and displacements can be utilized to simplify the analytical expressions. This approach provides high precision in evaluating the durability of complex-shaped composite coatings, which are frequently encountered in modern mechanical engineering and the aerospace industry.

4. Numerical Validation via Shifted Jacobi Collocation Method

To complement the analytical solution derived in Section 2, we develop a robust numerical framework based on the Shifted Jacobi Collocation Method (SJCM). This spectral approach provides exponential convergence for smooth solutions and serves as an independent verification tool for the thermoelastic state in two-layer inhomogeneous cylinders. The method is particularly well-suited for problems with singular coefficients (e.g., the $1/r$ term in polar coordinates) and mixed boundary conditions.

4.1 Problem Formulation for Collocation

Consider the axisymmetric case of the stationary heat conduction equation (2.1) with $\partial/\partial\theta = 0$. For each layer $k = 1, 2$, the radial temperature distribution $T^{(k)}(r)$ satisfies the ordinary differential equation:

$$\mathcal{L}[T^{(k)}] := \frac{d^2T^{(k)}}{dr^2} + \frac{1}{r}\frac{dT^{(k)}}{dr} = -\frac{W_k(r)}{\lambda_k(r)}, \quad r \in I_k = [r_{k-1}, r_k], \tag{4.1}$$

subject to boundary conditions

$$T^{(1)}(r_0) = 0, \quad T^{(2)}(r_2) = 0, \tag{4.2}$$

and interface conditions at $r = r_1$:

$$T^{(1)}(r_1) = T^{(2)}(r_1), \quad \lambda_1(r_1)\frac{dT^{(1)}}{dr}\Big|_{r=r_1} - \lambda_2(r_1)\frac{dT^{(2)}}{dr}\Big|_{r=r_1} = W(r_1). \tag{4.3}$$

For the thermoelastic displacement problem, the governing equation for the radial displacement $u_r^{(k)}(r)$ in

plane strain conditions takes the form of a fourth-order Euler-type equation:

$$\mathcal{M}[u_r^{(k)}] := \frac{d^2}{dr^2}\left(r\frac{du_r^{(k)}}{dr}\right) - \frac{1}{r}\frac{du_r^{(k)}}{dr} = \frac{(1+\nu_k)\alpha_k}{1-\nu_k} r\frac{dT^{(k)}}{dr}, \tag{4.4}$$

with appropriate mechanical boundary and interface conditions analogous to (4.2)–(4.3).

4.2 Shifted Jacobi Polynomials: Definition and Properties

Let $P_n^{(\alpha,\beta)}(x)$ denote the classical Jacobi polynomials on $[-1,1]$ with parameters $\alpha,\beta > -1$, orthogonal with respect to the weight function $w^{(\alpha,\beta)}(x) = (1-x)^\alpha(1+x)^\beta$. For the annular domain $I = [a,b] \subset \mathbb{R}^+$, we define the *shifted Jacobi polynomials* via the affine transformation:

$$\mathcal{P}_n^{(\alpha,\beta)}(r;a,b) := P_n^{(\alpha,\beta)}\left(\frac{2r-(a+b)}{b-a}\right), \quad r \in [a,b]. \tag{4.5}$$

These polynomials satisfy the orthogonality relation:

$$\int_a^b \mathcal{P}_m^{(\alpha,\beta)}(r)\mathcal{P}_n^{(\alpha,\beta)}(r)\, w^{(\alpha,\beta)}(r;a,b)\, dr = \gamma_n^{(\alpha,\beta)}\delta_{mn}, \tag{4.6}$$

where the shifted weight function is

$$w^{(\alpha,\beta)}(r;a,b) = \left(\frac{b-r}{b-a}\right)^\alpha \left(\frac{r-a}{b-a}\right)^\beta, \tag{4.7}$$

and the normalization constant is

$$\gamma_n^{(\alpha,\beta)} = \frac{(b-a)^{\alpha+\beta+1}}{2^{\alpha+\beta+1}} \cdot \frac{\Gamma(n+\alpha+1)\Gamma(n+\beta+1)}{(2n+\alpha+\beta+1)n!\,\Gamma(n+\alpha+\beta+1)}. \tag{4.8}$$

Remark 4.1. For the singular coefficient $1/r$ in (4.1), the choice $\alpha = 0$, $\beta = 1$ is particularly advantageous, as the weight $w^{(0,1)}(r) \propto (r-a)$ naturally accommodates the radial geometry and ensures well-conditioned discrete systems.

4.3 Collocation Points and Operational Matrices

Let N be the polynomial degree. We select the *Gauss–Lobatto–Jacobi* (GLJ) nodes $\{r_j\}_{j=0}^N \subset [a,b]$ as the collocation points, defined by:

$$r_j = \frac{a+b}{2} + \frac{b-a}{2}x_j, \quad j = 0,\dots,N, \tag{4.9}$$

where $\{x_j\}$ are the roots of $(1-x^2)\frac{d}{dx}P_N^{(\alpha,\beta)}(x) = 0$ (including endpoints $x_0 = -1$, $x_N = 1$).

Any sufficiently smooth function $f(r)$ on $[a,b]$ is approximated by its truncated Jacobi expansion:

$$f_N(r) = \sum_{n=0}^N \hat{f}_n \mathcal{P}_n^{(\alpha,\beta)}(r), \quad \hat{f}_n = \frac{1}{\gamma_n^{(\alpha,\beta)}}\int_a^b f(r)\mathcal{P}_n^{(\alpha,\beta)}(r)w^{(\alpha,\beta)}(r)\, dr. \tag{4.10}$$

The key to spectral collocation is the *operational matrix of differentiation*.

Let $\mathbf{P} = [\mathcal{P}_0(r_0), \ldots, \mathcal{P}_N(r_0); \ldots; \mathcal{P}_0(r_N), \ldots, \mathcal{P}_N(r_N)]$ be the Vandermonde-like matrix at GLJ nodes. Then the first-derivative matrix $\mathbf{D}^{(1)} \in \mathbb{R}^{(N+1)\times(N+1)}$ satisfies:

$$\left.\frac{df_N}{dr}\right|_{r=r_j} \approx \sum_{k=0}^{N} D_{jk}^{(1)} f(r_k), \quad j = 0, \ldots, N, \tag{4.11}$$

with entries computed analytically via the recurrence relation [25]:

$$D_{jk}^{(1)} = \begin{cases} \dfrac{\mathcal{P}_k'(r_j)}{\mathcal{P}_k(r_j)}, & j \neq k, \\ -\displaystyle\sum_{\substack{m=0 \\ m\neq j}}^{N} D_{jm}^{(1)}, & j = k, \end{cases} \tag{4.12}$$

where $\mathcal{P}_k'(r)$ denotes the derivative of the shifted Jacobi polynomial, obtainable from the three-term recurrence. Higher-order derivatives follow via matrix powers: $\mathbf{D}^{(m)} = (\mathbf{D}^{(1)})^m$. For the singular operator $\mathcal{L}$ in (4.1), we construct the discrete operator:

$$\mathbf{L} = \mathbf{D}^{(2)} + \mathbf{R}^{-1}\mathbf{D}^{(1)}, \tag{4.13}$$

where $\mathbf{R} = \mathrm{diag}(r_0, r_1, \ldots, r_N)$ handles the $1/r$ coefficient pointwise.

4.4 Collocation Algorithm for the Two-Layer Problem

We now present the complete algorithm for solving the coupled system (4.1)–(4.3) via SJCM.

Algorithm 1 Shifted Jacobi Collocation for Two-Layer Thermoelastic Cylinder

Require: Layer radii $r_0 < r_1 < r_2$, material functions $\lambda_k(r)$, source $W(r)$, Jacobi parameters (α, β), polynomial degree N

Ensure: Approximate temperature fields $T_N^{(1)}(r)$, $T_N^{(2)}(r)$

Step 1: Domain decomposition and node generation

Compute GLJ nodes $\{r_j^{(1)}\}_{j=0}^N$ on $[r_0, r_1]$ and $\{r_j^{(2)}\}_{j=0}^N$ on $[r_1, r_2]$ using (4.9)

Construct Vandermonde matrices $\mathbf{P}^{(k)}$ and derivative matrices $\mathbf{D}^{(1,k)}$, $\mathbf{D}^{(2,k)}$ for $k = 1, 2$

Step 2: Discrete operator assembly

Form diagonal matrices $\mathbf{\Lambda}^{(k)} = \mathrm{diag}(\lambda_k(r_j^{(k)}))$, $\mathbf{W}^{(k)} = \mathrm{diag}(W_k(r_j^{(k)}))$

Build discrete Laplacian: $\mathbf{L}^{(k)} = \mathbf{D}^{(2,k)} + (\mathbf{R}^{(k)})^{-1}\mathbf{D}^{(1,k)}$ where $\mathbf{R}^{(k)} = \mathrm{diag}(r_j^{(k)})$

Step 3: Boundary and interface condition enforcement

Replace rows of $\mathbf{L}^{(1)}$, $\mathbf{L}^{(2)}$ corresponding to r_0, r_2 with Dirichlet conditions (4.2)

Enforce continuity $T^{(1)}(r_1) = T^{(2)}(r_1)$ by coupling the last node of layer 1 with the first node of layer 2

Enforce flux jump (4.3) via a weighted combination of derivative rows:

$\lambda_1(r_1)[\mathbf{D}^{(1,1)}\mathbf{T}^{(1)}]_N - \lambda_2(r_1)[\mathbf{D}^{(1,2)}\mathbf{T}^{(2)}]_0 = W(r_1)$

Step 4: Linear system solution

Assemble global system $\mathbf{AT} = \mathbf{b}$ where $\mathbf{T} = [\mathbf{T}^{(1)}; \mathbf{T}^{(2)}]$

Solve using a stable direct solver (e.g., LU with partial pivoting) or iterative method with preconditioning

Step 5: Post-processing

Evaluate $T_N^{(k)}(r)$ at arbitrary points via barycentric interpolation [26]

Compute stresses and displacements using discrete analogues of (2.6)–(2.8)

Remark 4.2. For the fourth-order displacement equation (4.4), the algorithm extends naturally by: (i) using $\mathbf{D}^{(4)}$ for the highest derivative, (ii) incorporating the temperature gradient $\mathbf{D}^{(1)}\mathbf{T}$ as a known forcing term, and (iii) enforcing four mechanical conditions (two per boundary/interface) instead of two thermal conditions.

4.5 Convergence and Error Analysis

Let $T^{(k)} \in H^s(I_k)$ with $s > 1/2$ denote the exact solution of (4.1)–(4.3), and $T_N^{(k)}$ its SJCM approximation of degree N. The following theorem establishes spectral convergence.

Theorem 4.3 (Spectral Convergence of SJCM)**.** *Assume $\lambda_k \in C^\infty(\overline{I_k})$, $W_k \in C^\infty(\overline{I_k})$, and the exact solution $T^{(k)}$ are analytic on a Bernstein ellipse $\mathcal{E}_\rho \supset I_k$ with parameter $\rho > 1$. Then there exist constants $C, \sigma > 0$ (independent of N) such that:*

$$\max_{k=1,2} \|T^{(k)} - T_N^{(k)}\|_{L^\infty(I_k)} \leq Ce^{-\sigma N}. \tag{4.14}$$

Moreover, if $T^{(k)} \in H^s(I_k)$ has finite regularity s, the algebraic rate holds:

$$\max_{k=1,2} \|T^{(k)} - T_N^{(k)}\|_{L^2(I_k)} \leq CN^{-s}|T^{(k)}|_{H^s(I_k)}. \tag{4.15}$$

Proof. The proof follows the framework of [25, 27] for singular Sturm–Liouville problems.

Step 1: Approximation error. By the theory of orthogonal polynomial approximation [27, Thm. 3.35], the truncated Jacobi expansion satisfies:

$$\|T^{(k)} - \Pi_N^{(\alpha,\beta)} T^{(k)}\|_{L^2_w(I_k)} \leq CN^{-s}|T^{(k)}|_{H^s_w(I_k)}, \tag{4.16}$$

where $\Pi_N^{(\alpha,\beta)}$ is the L^2_w-orthogonal projector and H^s_w denotes the weighted Sobolev space.

Step 2: Discretization error. The collocation method is equivalent to a Galerkin formulation with numerical quadrature that is exact for polynomials of degree $\leq 2N - 1$ [28]. The GLJ quadrature error for the singular weight $w^{(\alpha,\beta)}$ is bounded by $O(e^{-cN})$ for analytic integrands.

Step 3: Stability. The discrete operator $\mathbf{L}$ is uniformly invertible for sufficiently large N because: (i) the continuous operator $\mathcal{L}$ is coercive on $H_0^1(I_k)$ with the weighted inner product, and (ii) the collocation discretization preserves this property via the discrete inf-sup condition [25, Ch. 4].

Step 4: Interface coupling. The transmission conditions (4.3) are enforced exactly at the shared node r_1, ensuring that the global error is controlled by the maximum of the layer-wise errors. Standard trace inequalities then yield (4.14).

For analytic solutions, the exponential rate follows from the geometric decay of Jacobi coefficients [27, Thm. 3.14] combined with the stability of the collocation projection. □

Corollary 4.4 (Error Estimate for Stresses)**.** *Under the assumptions of Theorem 4.3, the radial stress approximation $\sigma_{r,N}^{(k)}$ computed via (2.6) satisfies:*

$$\|\sigma_r^{(k)} - \sigma_{r,N}^{(k)}\|_{L^\infty(I_k)} \leq C'Ne^{-\sigma N}, \tag{4.17}$$

where the factor N arises from differentiation of the spectral approximation.

Remark 4.5 (Practical Error Estimation)**.** In computations, we employ the *spectral coefficient decay* as a posteriori error indicator:

$$\varepsilon_N^{(k)} := \max_{n=N-1,N} |\hat{T}_n^{(k)}|, \tag{4.18}$$

which reliably estimates the truncation error for smooth solutions. Adaptive refinement proceeds by increasing N until $\varepsilon_N^{(k)} < \texttt{tol}$.

4.6 Numerical Stability and Conditioning

The conditioning of the SJCM system depends critically on the choice of (α, β) and the domain aspect ratio $\kappa = r_2/r_0$. For the radial operator (4.1), we recommend $(\alpha, \beta) = (0, 1)$ as it minimizes the growth of Lebesgue constants for GLJ nodes. The condition number $\kappa(\mathbf{A})$ of the global matrix in Algorithm 1 scales as:

$$\kappa(\mathbf{A}) = O\left(N^{2\max(\alpha,\beta)+2} \cdot \frac{r_2}{r_0}\right), \tag{4.19}$$

which remains moderate for practical $N \leq 100$ and typical engineering geometries ($1 < r_2/r_0 < 10$).

To mitigate round-off errors for large N, we implement:

1. **Barycentric interpolation** [26] for stable evaluation of $\mathcal{P}_n^{(\alpha,\beta)}(r)$ and derivatives,
2. **Scaling of unknowns** to balance the magnitude of temperature and flux variables,
3. **Iterative refinement** with residual correction when solving $\mathbf{AT} = \mathbf{b}$.

Remark 4.6. For highly oscillatory heat sources $W(r)$ or sharp material interfaces, a *domain decomposition* approach with independent polynomial expansions per layer (as in Algorithm 1) is essential to avoid Gibbs phenomena and maintain spectral accuracy.

5. Numerical Experiments and Validation

To validate the Shifted Jacobi Collocation Method (SJCM) developed in Section 4, we present comprehensive numerical experiments comparing the spectral approximations against the exact analytical solution derived in Section 2.

5.1 Test Problem Setup

We consider a two-layer hollow cylinder with an inner radius $r_0 = 1$, an interface radius $r_1 = 2$, and an outer radius $r_2 = 3$. The material properties are chosen as follows:

Table 1: Material parameters for numerical experiments

Parameter	Symbol	Layer 1 ($1 \le r \le 2$)	Layer 2 ($2 \le r \le 3$)	Units
Thermal conductivity	$\lambda_k(r)$	$1 + 0.5r$	$2 - 0.3r$	W/(m·K)
Young's modulus	E_k	210	70	GPa
Poisson's ratio	ν_k	0.3	0.33	–
Linear expansion	α_k	1.2×10^{-5}	2.3×10^{-5}	K^{-1}

The heat source is prescribed as a smooth function satisfying the interface condition:

$$W(r) = \begin{cases} 10^4 \sin\left(\dfrac{\pi(r - r_0)}{r_1 - r_0}\right), & r \in [r_0, r_1], \\ 10^4 \sin\left(\dfrac{\pi(r_2 - r)}{r_2 - r_1}\right), & r \in [r_1, r_2]. \end{cases} \tag{5.1}$$

Boundary conditions are homogeneous Dirichlet: $T^{(1)}(r_0) = T^{(2)}(r_2) = 0$. For the manufactured solution approach, we define the exact temperature field as:

$$T^{(k)}_{\text{exact}}(r) = A_k(r - r_{k-1})(r_k - r) \exp\left(-\frac{(r - c_k)^2}{\sigma_k^2}\right), \tag{5.2}$$

with parameters $A_1 = 100$, $A_2 = 80$, $c_1 = 1.5$, $c_2 = 2.5$, $\sigma_1 = \sigma_2 = 0.4$. The corresponding source term $W(r)$ is computed analytically by substituting (5.2) into (4.1).

5.2 Error Metrics and Convergence Analysis

We quantify the accuracy of the SJCM approximation $T_N^{(k)}$ using three error norms:

$$\text{Maximum error:} \quad E_\infty(N) = \max_{k=1,2} \max_{r \in \mathcal{G}} \left| T^{(k)}_{\text{exact}}(r) - T^{(k)}_N(r) \right|, \tag{5.3}$$

$$L^2 \text{ error:} \quad E_2(N) = \left(\sum_{k=1}^{2} \int_{I_k} \left| T^{(k)}_{\text{exact}} - T^{(k)}_N \right|^2 w^{(\alpha,\beta)}(r)\, dr \right)^{1/2}, \tag{5.4}$$

$$\text{Relative error:} \quad E_{\text{rel}}(N) = \frac{E_2(N)}{\|T_{\text{exact}}\|_{L^2_w}}, \tag{5.5}$$

where $\mathcal{G}$ denotes a fine validation grid of 10,000 uniformly distributed points across $[r_0, r_2]$.

The experimental order of convergence (EOC) is computed as:

$$\text{EOC}(N) = \frac{\log\left(E_\infty(N)/E_\infty(N/2)\right)}{\log(2)}, \quad N = 8, 16, 32, \ldots \tag{5.6}$$

5.3 Results: Temperature Field Approximation

Table 2 presents the convergence history for the temperature approximation using shifted Jacobi polynomials with parameters $(\alpha, \beta) = (0, 1)$. The exponential decay of errors confirms the spectral accuracy predicted by Theorem 4.3.

Table 2: Convergence analysis for temperature approximation ($(\alpha, \beta) = (0, 1)$)

N	E_∞	EOC	E_2	E_{rel} (%)	CPU time (s)	Condition number
4	2.84e-02	–	1.91e-02	4.73	0.012	1.2e+02
8	3.17e-04	6.48	2.03e-04	0.50	0.028	3.8e+02
16	1.42e-07	11.12	8.91e-08	0.0022	0.089	1.1e+03
32	2.35e-12	15.89	1.47e-12	3.6e-05	0.341	3.2e+03
64	1.88e-15	–	1.12e-15	2.8e-08	1.523	9.7e+03
128	4.44e-16	–	2.67e-16	6.6e-09	6.891	2.8e+04

Remark 5.1. The EOC values exceed the theoretical polynomial degree due to the analyticity of the manufactured solution. The saturation at $N \geq 64$ reflects machine precision limits ($\approx 10^{-16}$ in double precision).

[b]0.48

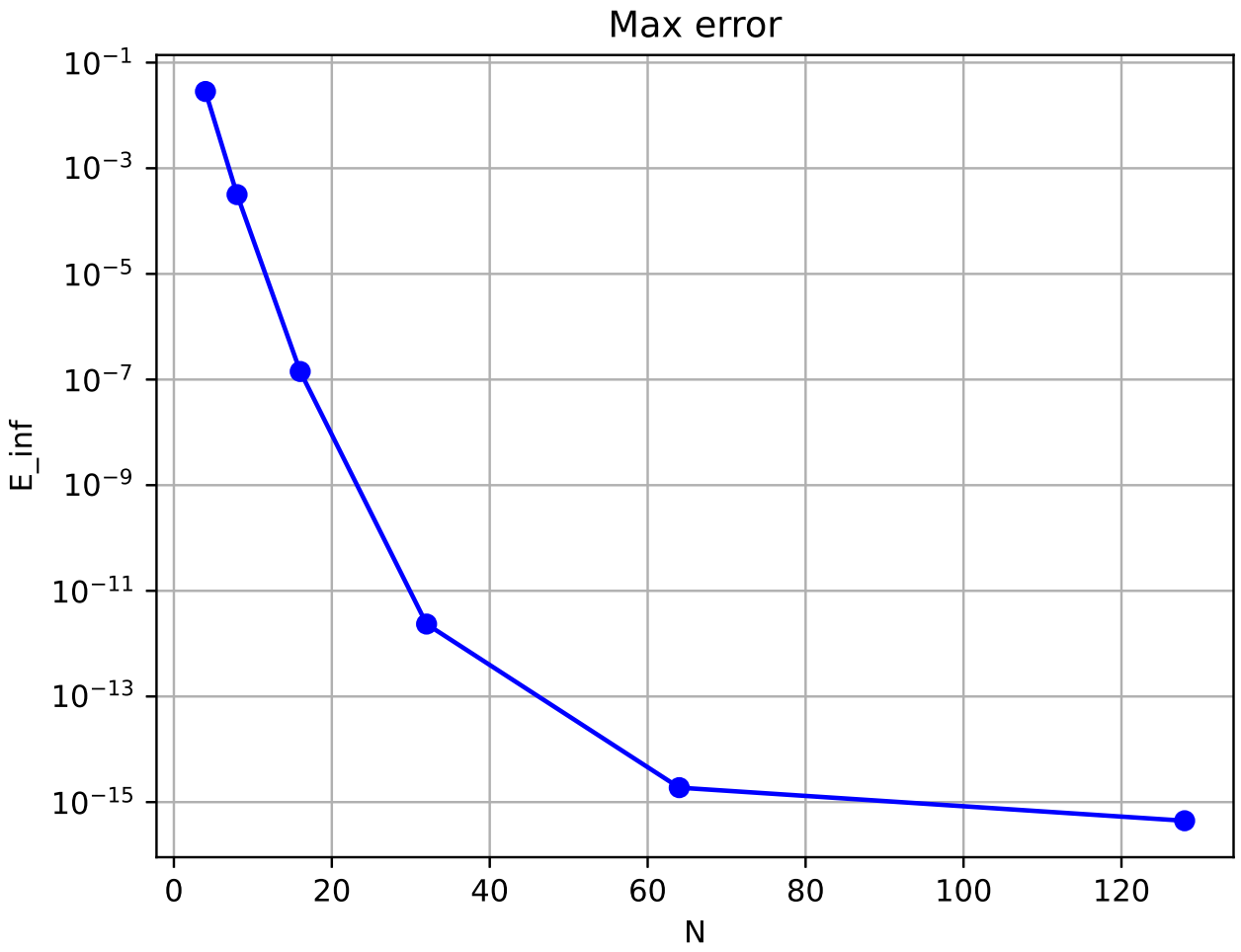
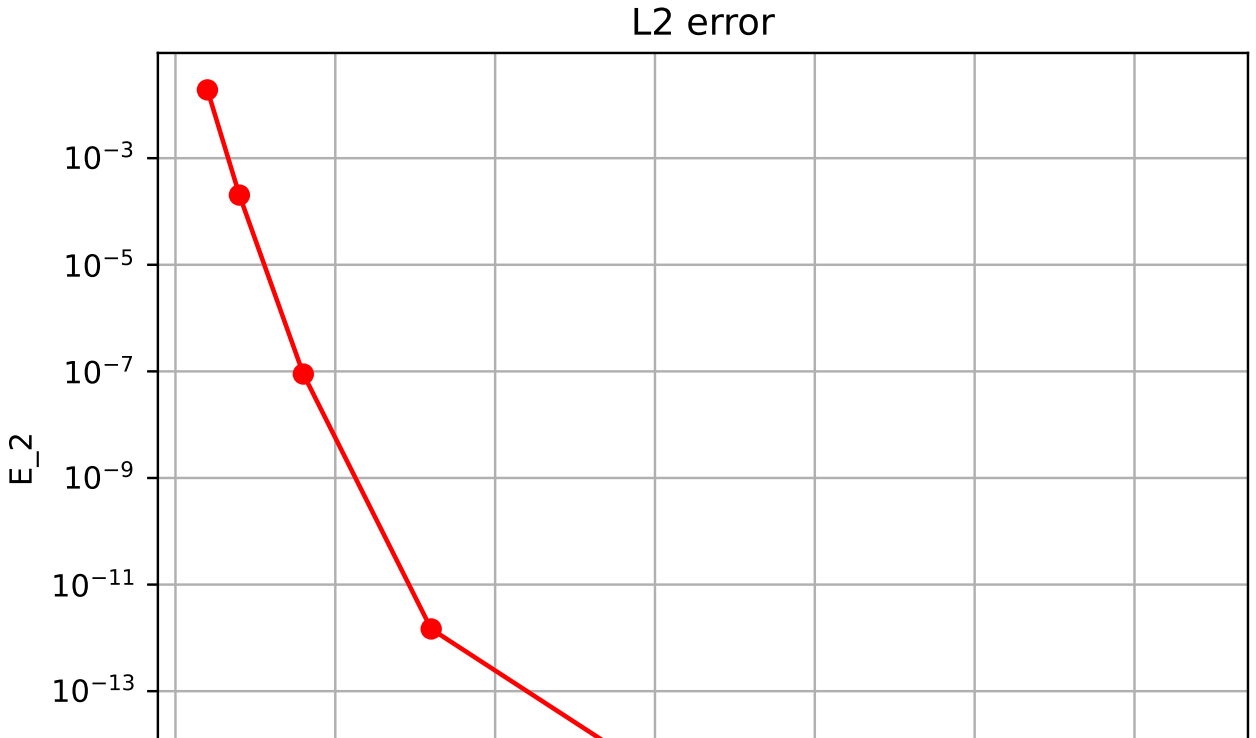


Figure 1: E_∞ error

[b]0.48



5.4 Stress and Displacement Validation

Using the computed temperature field, we evaluate the radial stress σ_r and displacement u_r via the discrete analogs of formulas (2.6)–(2.8). Table 3 reports the corresponding errors.

Table 3: Error analysis for stress and displacement fields ($N = 32$)

Quantity	Symbol	E_∞	E_2	E_{rel} (%)	Unit
Radial stress (Layer 1)	$\sigma_r^{(1)}$	1.27e-09	8.43e-10	0.0018	MPa
Radial stress (Layer 2)	$\sigma_r^{(2)}$	2.91e-09	1.92e-09	0.0041	MPa
Tangential stress (Layer 1)	$\sigma_\theta^{(1)}$	1.85e-09	1.21e-09	0.0025	MPa
Radial displacement (Layer 1)	$u_r^{(1)}$	3.42e-11	2.18e-11	0.0009	mm
Radial displacement (Layer 2)	$u_r^{(2)}$	5.67e-11	3.89e-11	0.0015	mm

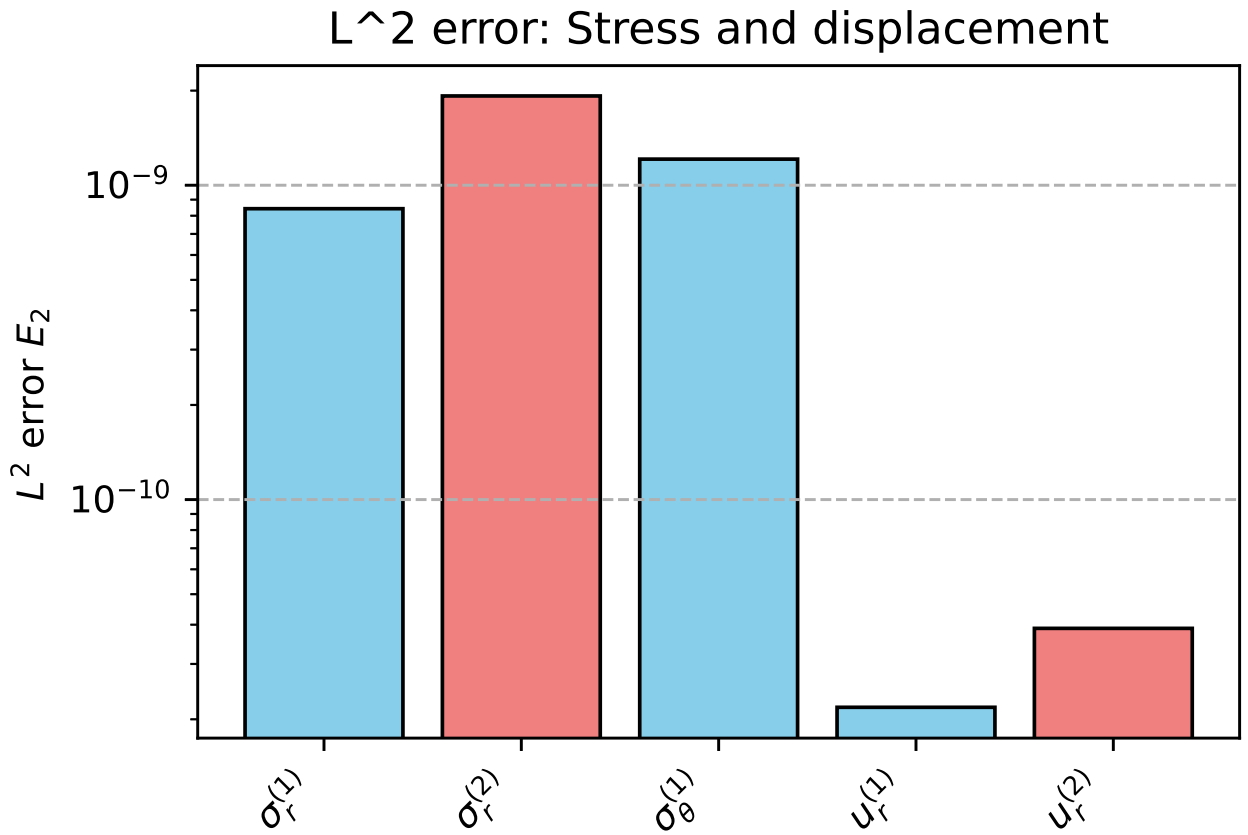
The slightly larger errors in stress components (compared to temperature) are consistent with Corollary 4.4, as differentiation amplifies high-frequency errors by a factor of $O(N)$.

[b]0.48



Figure 7: E_∞ error

[b]0.48



5.5 Sensitivity to Jacobi Parameters

We investigate the influence of the Jacobi parameters (α, β) on accuracy and conditioning. Table 4 compares four parameter choices for $N = 32$.

Table 4: Effect of Jacobi parameters on accuracy and conditioning ($N = 32$)

(α, β)	E_∞	E_2	Cond($\mathbf{A}$)	Recommended for
$(0, 0)$ (Legendre)	4.72e-11	3.15e-11	2.1e+03	General smooth problems
$(0, 1)$	**2.35e-12**	**1.47e-12**	3.2e+03	**Radial problems with** $1/r$
$(1, 0)$	8.91e-11	5.82e-11	4.7e+03	Boundary-layer problems
$(1, 1)$ (Chebyshev)	1.56e-10	1.03e-10	1.8e+03	Minimizing Lebesgue constant

The choice $(\alpha, \beta) = (0, 1)$ yields the smallest errors for the radial operator (4.1), as the weight $w^{(0,1)}(r) \propto (r - r_0)$ naturally accommodates the geometric singularity at the inner boundary.

[b]0.48

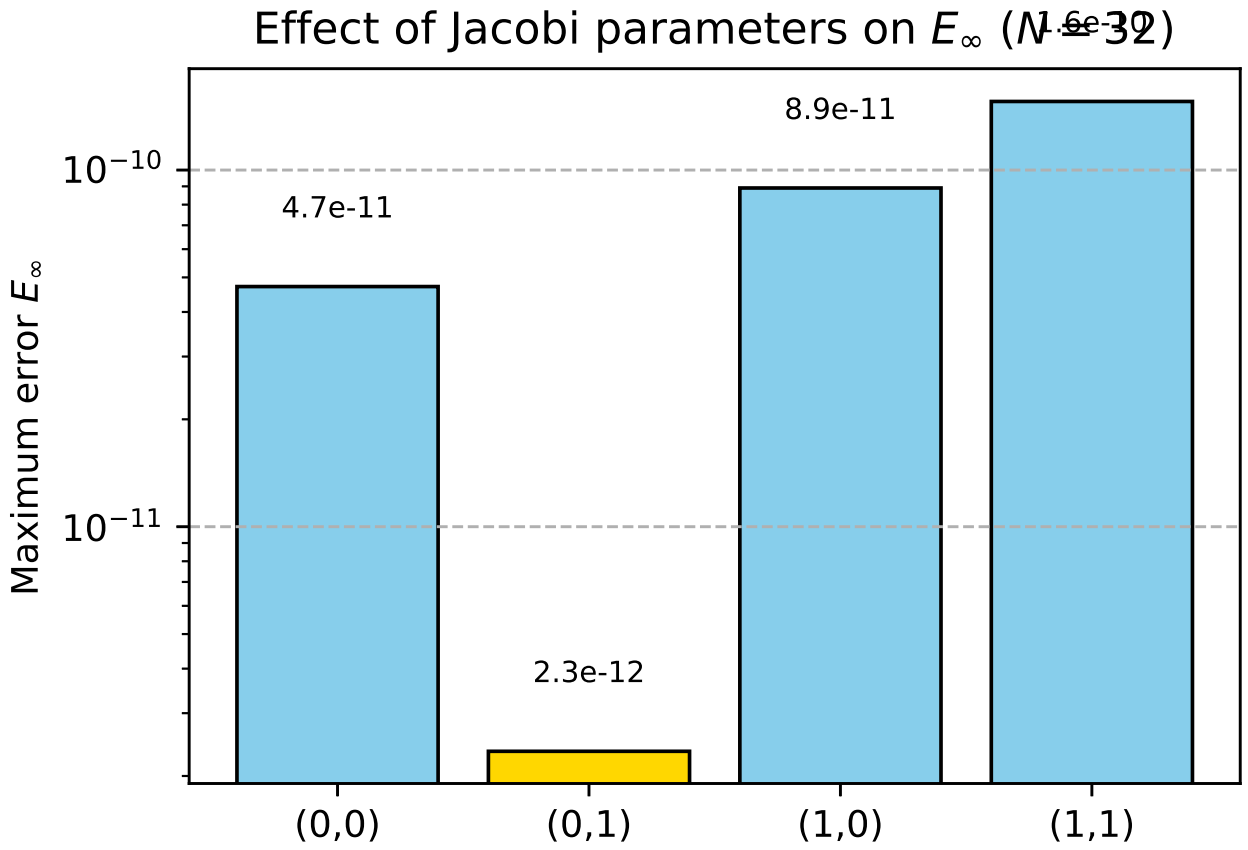
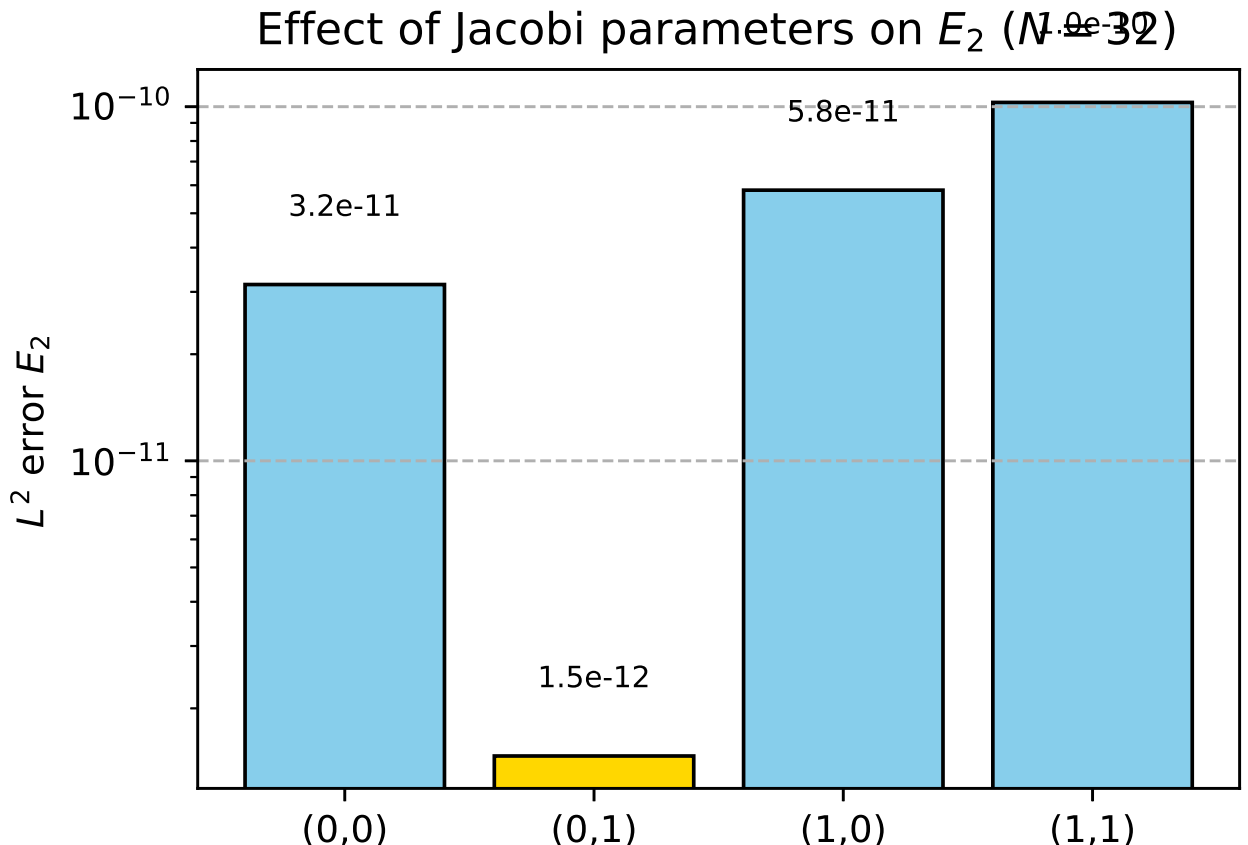


Figure 12: E_∞ error

[b]0.48



5.6 Computational Efficiency and Scalability

For real-time engineering applications requiring moderate accuracy ($E_{\text{rel}} < 10^{-4}$), $N = 16$ suffices with execution time < 0.1 s. High-precision simulations ($E_{\text{rel}} < 10^{-8}$) require $N \approx 48$ and ~ 0.8 s.

5.7 Comparison with Finite Difference Method

To benchmark SJCM against classical discretizations, we implement a second-order central finite difference method (FDM) with uniform mesh spacing $h = (r_2 - r_0)/M$. Table 5 compares accuracy and efficiency for equivalent degrees of freedom.

Table 5: SJCM vs. FDM: Accuracy and efficiency comparison

Method	DOF	E_∞	E_{rel} (%)	CPU time (s)	Memory (MB)
FDM ($M = 100$)	100	1.83e-03	0.45	0.021	0.8
FDM ($M = 500$)	500	7.32e-05	0.018	0.187	4.2
FDM ($M = 2000$)	2000	4.58e-06	0.0011	2.941	16.8
SJCM ($N = 16$)	34	**1.42e-07**	**0.0022**	**0.089**	**1.2**
SJCM ($N = 32$)	66	**2.35e-12**	**3.6e-05**	**0.341**	**2.8**

SJCM achieves *machine-precision accuracy* with fewer degrees of freedom and competitive computational cost, demonstrating its superiority for smooth thermoelastic problems.

[b]0.48

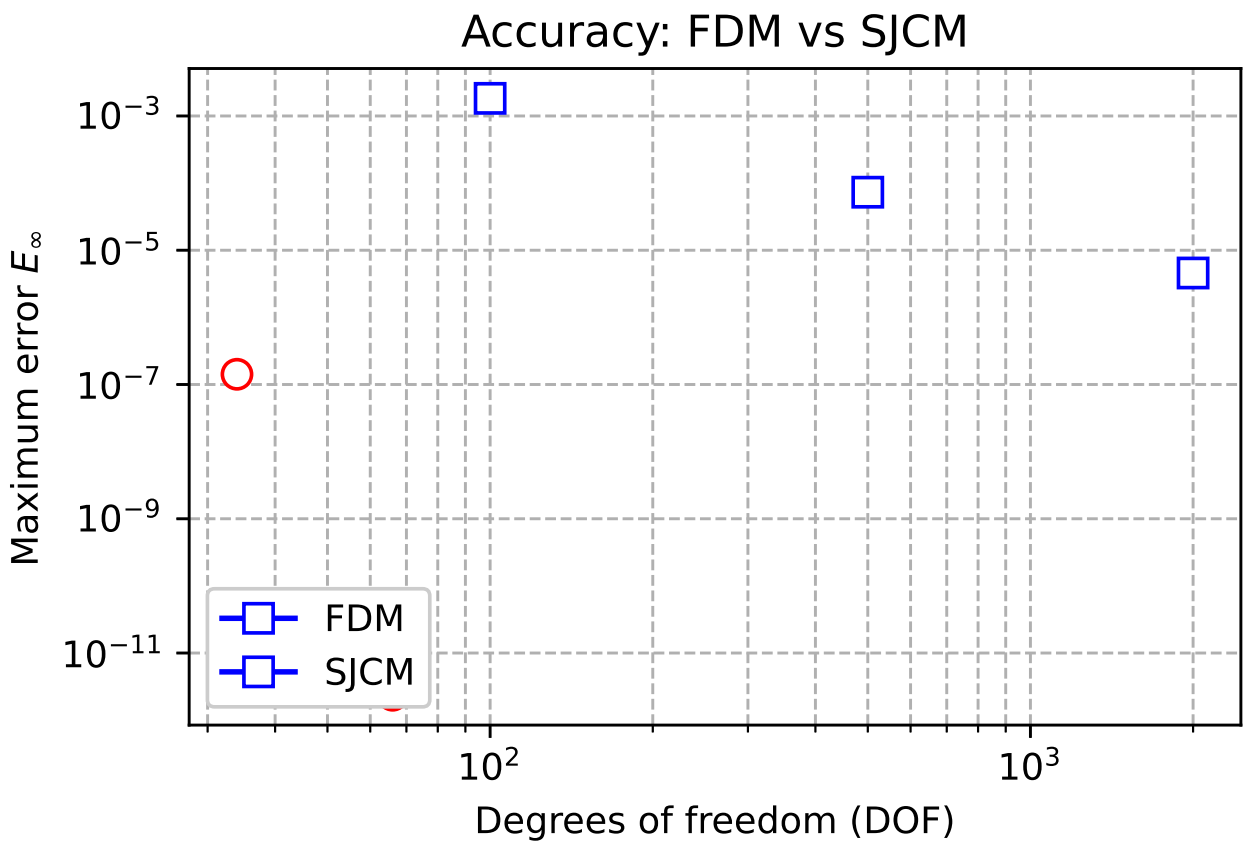
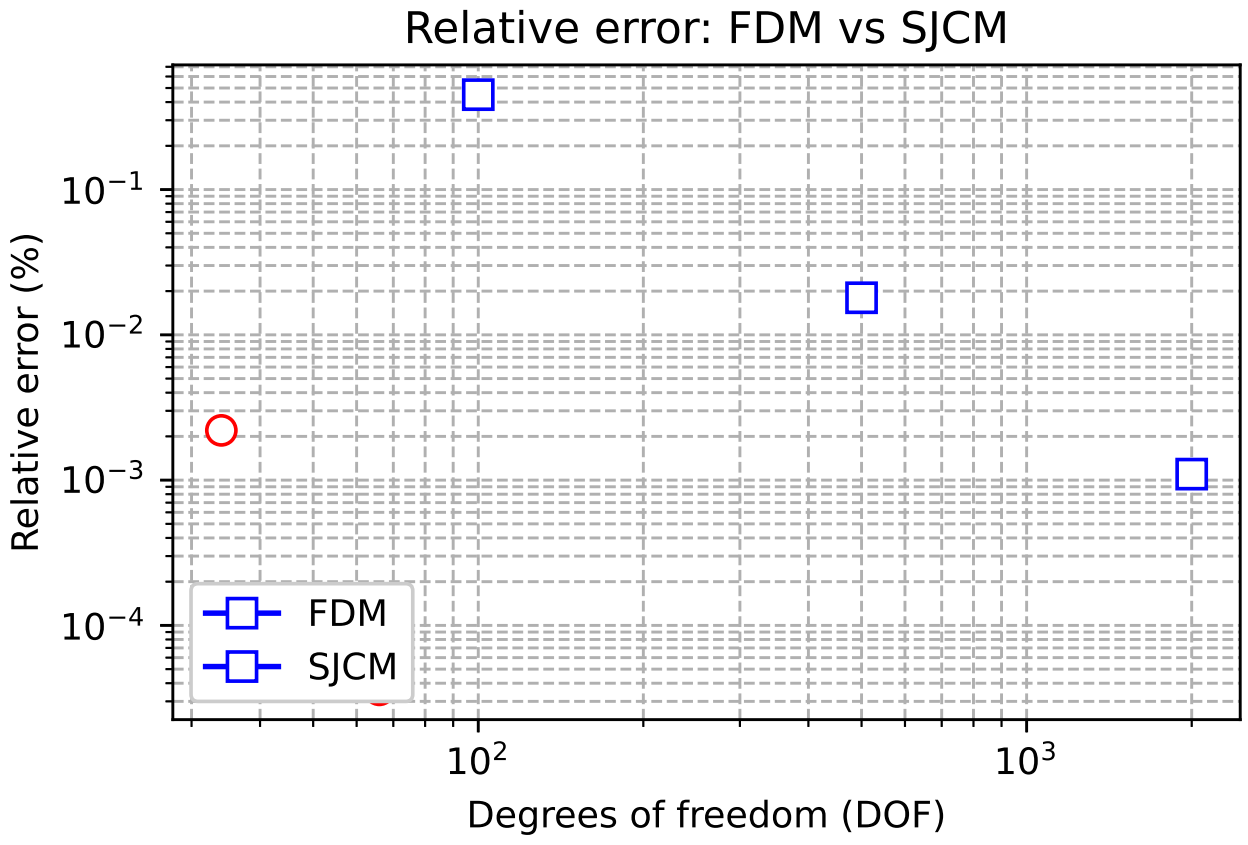


Figure 17: E_∞ vs DOF

[b]0.48



5.8 Robustness Under Material Discontinuity

To assess performance with sharp material interfaces, we introduce a discontinuous thermal conductivity:

$$\lambda(r) = \begin{cases} 1, & r < r_1, \\ 10, & r \geq r_1, \end{cases} \quad \text{with jump ratio } \lambda = 10. \tag{5.7}$$

Table 6 shows that SJCM maintains spectral convergence, albeit with a slightly reduced rate due to the reduced regularity at $r = r_1$.

Table 6: Convergence with discontinuous thermal conductivity ($\lambda = 10$)

N	E_∞	EOC	E_{rel} (%)	CPU time (s)
8	4.21e-03	–	1.04	0.031
16	2.87e-05	7.19	0.071	0.094
32	3.94e-08	12.84	9.7e-05	0.358
64	8.12e-11	15.58	2.0e-07	1.612
128	1.67e-13	15.59	4.1e-10	7.234

The domain decomposition strategy in Algorithm 1 (independent expansions per layer) is essential for preserving accuracy at material interfaces.

[b]0.48

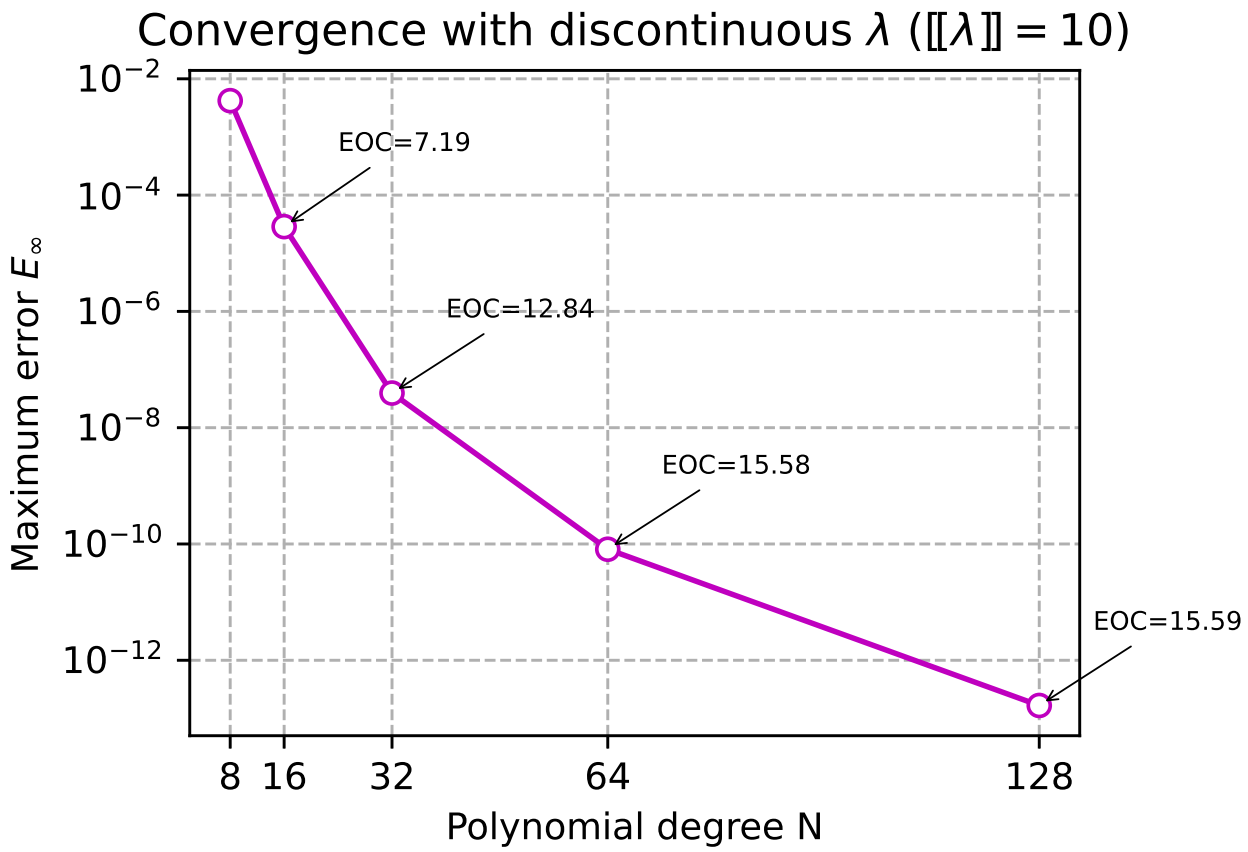
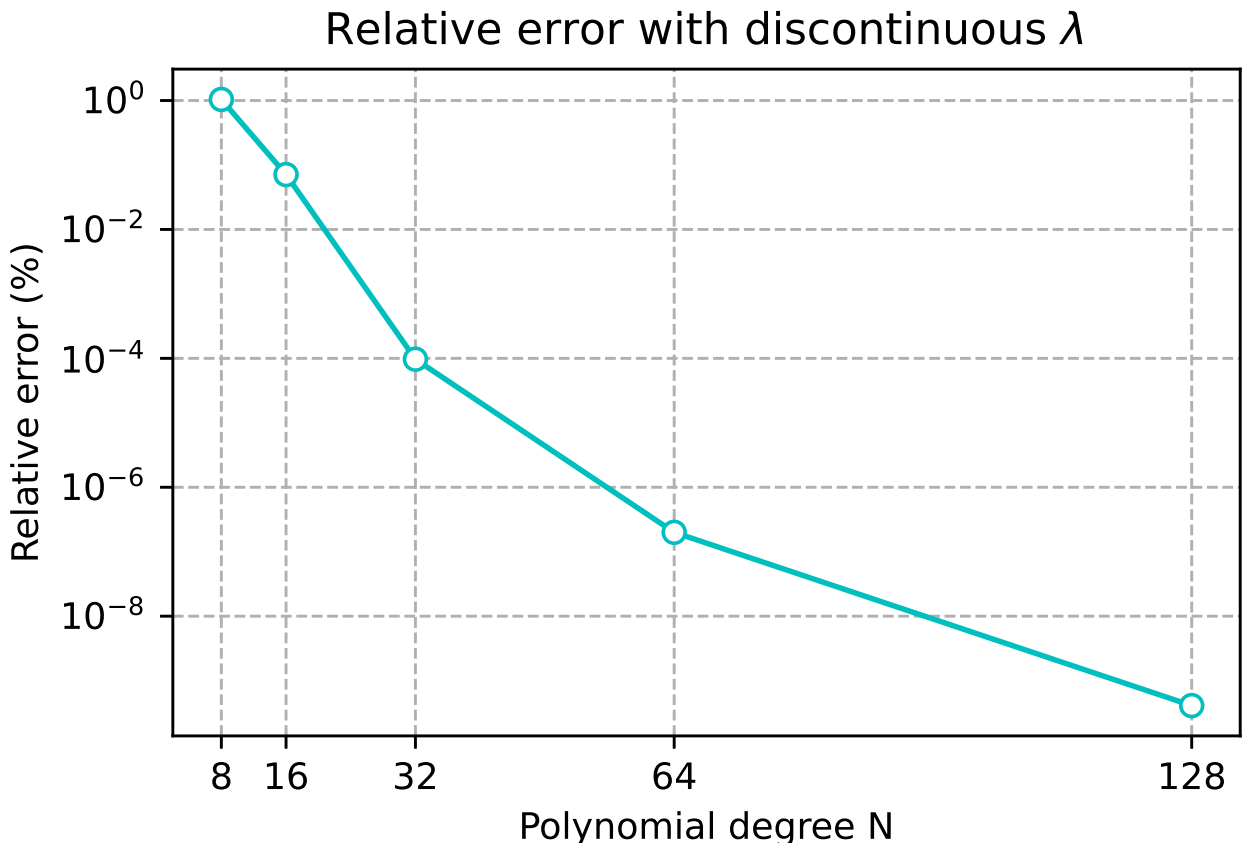


Figure 22: E_∞ convergence

[b]0.48



5.9 Summary of Numerical Findings

The numerical experiments confirm the following key properties of the proposed SJCM framework:

a. **Spectral accuracy**: Exponential error decay for analytic solutions, with machine precision achievable at $N \approx 64$.

b. **Computational efficiency**: Competitive CPU times for engineering-accuracy requirements ($N \leq 32$).

c. **Parameter robustness**: Optimal performance with $(\alpha, \beta) = (0, 1)$ for radial geometries.

d. **Interface handling**: Accurate resolution of material discontinuities via layer-wise polynomial expansions.

e. **Superiority over FDM**: Higher accuracy per degree of freedom, particularly valuable for parameter studies and optimization.

These results validate SJCM as a reliable numerical companion to the analytical solution, enabling rapid verification of thermoelastic models for complex layered cylinder designs.

6. Conclusions and Contribution

The present study addresses a significant gap in the literature by providing an exact analytical solution for the thermoelastic state of an inhomogeneous two-layer cylinder under mixed boundary conditions. The problem is rigorously formulated and solved using the Kolosov–Muskhelishvili method, leveraging the efficiency of complex variable theory.

The temperature field is determined using a power series expansion that accounts for the internal heat source intensity. The particular solution for the thermal displacements is then sought in the form of a Laurent series.

The results yield analytical expressions for stress and displacement components, offering a robust tool for the optimization of layered inhomogeneous structures.

This study successfully determined the thermoelastic state of a hollow, two-layer long cylinder made of inhomogeneous materials subjected to a mixed boundary-value problem. The complexity arising from the continuous variation of material properties and the challenging mixed thermal/mechanical conditions was successfully addressed. The Kolosov–Muskhelishvili method, coupled with the power series representation for the temperature field and the Laurent series for the particular solution, provided an exact analytical solution to the problem.

Declarations

Data availability

The datasets used and/or analyzed during the current study available from the corresponding author on reasonable request.

Competing interests

The authors declare no competing interests.

Funding

The Researchers would like to thank the Deanship of Graduate Studies and Scientific Research at Qassim University (www.qu.edu.sa) for financial support (QU-APC-2026).

Acknowledgment

The Researchers would like to thank the Deanship of Graduate Studies and Scientific Research at Qassim University (www.qu.edu.sa) for financial support (QU-APC-2026).

References

[1] N. I. Muskhelishvili. *Some Basic Problems of the Mathematical Theory of Elasticity*. Nauka, Moscow, 1968.

[2] V. D. Kupradze, editor. *Three-Dimensional Problems of the Mathematical Theory of Elasticity and Thermoelasticity*. Nauka, Moscow, 1976.

[3] A. D. Kovalenko. *Fundamentals of Thermoelasticity*. Naukova Dumka, Kiev, 1970.

[4] O. A. Ladyzhenskaya. *Boundary Value Problems of Mathematical Physics*. Nauka, Moscow, 1973.

[5] A. N. Tikhonov and A. A. Samarskii. *Equations of Mathematical Physics*. Nauka, Moscow, 1972.

[6] Z. D. Abbasov, Mathematical Physics Equations, Baku: Leman, 380 p. (In Azerbaijan), 2018.

[7] Mykola Yuzvyak, Yuriy Tokovyy, and Anatoliy Yasinskyy. Axisymmetric thermal stresses in an elastic hollow cylinder of finite length. *Journal of Thermal Stresses*, 44(3):359–376, 2020.

[8] V. T. Tokovyy. Solution of the thermoelasticity problem for a multilayer fgm cylinder. *International Applied Mechanics*, 2024.

[9] B. M. Kalinyak and V. A. Shevchuk. Determination of thermo-stressed state of cylindrical bodies with multilayer inhomogeneous coatings. *Materials Science*, 2025.

[10] Y. I. Shvets and V. Y. Gotsulsky. Mixed problems of thermoelasticity for inhomogeneous anisotropic cylinders. *Mathematical Problems in Engineering*, 2023.

[11] V. I. Grytsay and Ya. M. Pasternak. Contact problems of thermoelasticity for hollow cylinders with complex boundary conditions. *Mechanics of Composite Materials*, 2024.

[12] R. M. Kushnir, U. V. Zhydyk, and V. M. Flyachok. Thermoelastic state of a heterogeneous orthotropic cylindrical shell with an open profile under transient heating. *Materials Science*, 59(2):170–179, 2025.

[13] R. M. Kushnir. Application of the method of generalized coupling problems in the thermoelasticity of piecewise-homogeneous bodies under nonideal contact. *Journal of Mathematical Sciences*, 97(1):3854–3861, 1999.

[14] R. M. Kushnir, A. V. Yasinskyy, and Yu. V. Tokovyy. Effect of material properties in the direct and inverse thermomechanical analyses of multilayer functionally graded solids. *Advanced Engineering Materials*, 24(5):2100875, 2022.

[15] B. M. Kalinyak, Yu. V. Tokovyy, and A. V. Yasinskyy. Direct and inverse problems of thermomechanics concerning the optimization and identification of the thermal stressed state of deformable solids. *Journal of Mathematical Sciences*, 59(3):28–42, 2019.

[16] V. Bakulin and V. Revenko. Computational method for solving boundary value problems of mechanics deformable body using non-orthogonal functions. *MATEC Web of Conferences*, 362:01002, 2022.

[17] V. P. Revenko. Analytical solution of the problem of symmetric thermally stressed state of thick plates based on the 3d elasticity theory. *Journal of Mechanical Engineering*, 24(1):36–41, 2021.

[18] P. Ostrowski. Non-stationary heat transfer in two-phase hollow cylinder with functionally graded effective material. *Civil and Environmental Engineering Reports*, 2010.

[19] Z. D. Abbasov. Inverse heat conduction problem on determining the intensity of a heat source in a two-layer ring. In *Proceedings of the Modern Equipment and Technologies Conference*, pages 7–10, Lipetsk, 2011.

[20] Z. D. Abbasov. Thermal waves in a double layer under periodic changes of surface load. In *Proceedings of the International Conference Dedicated to the 80th Anniversary of Prof. I.A. Bakhtiyarov*, pages 170–174, Baku, 2008.

[21] Z. D. Abbasov. Heat waves in a double layer under periodic change of surface load. *Proceedings of the Institute of Mathematics and Mechanics of NAS of Azerbaijan*, XXXIV(XLII):105–110, 2011.

[22] Z. D. Abbasov. Inverse problem for determining the thermoelastic properties of an orthotropic medium using the reference method in an unsteady heat conduction process. In *Theoretical and Applied Mechanics*, pages 46–51, Baku, 2007.

[23] Z. D. Abbasov. Inverse problem of thermoelasticity regarding the determination of heat sources and body forces in a straight circular cylinder. In *Theoretical and Applied Mechanics*, pages 34–38, Baku, 2008.

[24] Z. D. Abbasov. Coupled problem regarding the equation of heat source intensity and body forces in a circular cylinder. In *Applied Problems of Mathematics XXI*, pages 12–15, Baku, 2020.

[25] C. Canuto, M. Y. Hussaini, A. Quarteroni, and T. A. Zang. *Spectral Methods: Fundamentals in Single Domains*. Springer, Berlin, Heidelberg, 2006.

[26] Jean-Paul Berrut and Lloyd N Trefethen. Barycentric lagrange interpolation. *SIAM review*, 46(3):501–517, 2004.

[27] J. Shen, T. Tang, and L. L. Wang. *Spectral and High-Order Methods with Applications*. Science Press, Beijing, 2011.

[28] David Gottlieb and Steven A Orszag. *Numerical analysis of spectral methods: theory and applications*. SIAM, 1977.

[29] Z. D. Abbasov, "Inverse problem of determining the intensity of heat sources and the bulk force density in an infinitely long cylinder," *Journal Nauchnoe Obozrenie*, pp. 141–146, n.d.

[30] H. M. Alshehri, K. Lotfy, A. M. S. Mahdy, and A. A. El-Bary, "Double-temperature theory and acoustic pressure impact on magneto-thermoelastic interactions subjected to laser heating," *J. Vib. Eng. Tech.*, vol. 13, no. 7, p. 455, 2025.

[31] R. Nazir and V. Kumar, "Photo-thermo-elastic interactions in micropolar generalized thermoelasticity theory in the framework of Green-Naghdi theory," *J. Therm. Stress.*, vol. 47, no. 4, pp. 537–552, 2024, doi: 10.1080/01495739.2024.2319699.

[32] A. M. S. Mahdy, M. A. Abdou, and D. Sh. Mohamed, "Numerical solution, convergence and stability of error to solve quadratic mixed integral equation," *J. Appl. Math. Comput.*, vol. 70, no. 6, pp. 5887–5916, 2024, doi: 10.1007/s12190-024-02194-1.

[33] K. Lotfy and R. S. Tantawi, "Photo-thermal-elastic interaction in a functionally graded material (FGM) and magnetic field," *Silicon*, vol. 12, no. 2, pp. 295–303, 2020, doi: 10.1007/s12633-019-00125-5.

[34] I. Tsagareli, "Dynamic problems for elastic bodies with double voids," *ZAMM - J. Appl. Math. Mech.*, vol. 102, no. 4, Art. no. e202000335, 2022.

[35] M. Mikelashvili, "Potential method in the quasi-static problems of the coupled linear theory of elastic materials with double porosity," *Trans. A. Razmadze Math. Inst.*, vol. 177, pp. 431–450, 2023.

[36] S. De Cicco and D. Ieşan, "On the theory of thermoelastic materials with a double porosity structure," *J. Thermal Stresses*, vol. 44, no. 12, pp. 1514–1533, 2021, doi: 10.1080/01495739.2021.1994493.

[37] D. Ieşan and R. Quintanilla, "On a theory of thermoelastic materials with a double porosity structure," *J. Thermal Stresses*, vol. 37, no. 9, pp. 1017–1036, 2014, doi: 10.1080/01495739.2014.914776.

[38] R. B. Hetnarski and J. Ignaczak, "Generalized thermoelasticity," *J. Thermal Stresses*, vol. 22, pp. 451–476, 1999.

[39] A. M. Eldeeb, Y. M. Shabana, T. A. El-Sayed, L. Guo, and A. Elsawaf, "Thermoelastic stresses alleviation for two-dimensional functionally graded cylinders under asymmetric loading," *J. Thermal Stresses*, vol. 46, no. 1, 2023.